PAPER

Check for updates

Fullerene-polysaccharide supramolecular hydrogel displaying antioxidation/antiglycation behavior†

Hong-Mei Yu,‡[ab] Xiao-Yong Yu,‡[c] Yong Chen[c] and Yu Liu [ID] *[c]

A fullerene-polysaccharide supramolecular hydrogel was constructed by carrying out a co-assembly of fullerene@hydroxypropyl-β-cyclodextrin, chitosan and bentonite, and displayed good antioxidant and antiglycation properties, and hence showed promising cosmetics applications. Benefitting from the cyclodextrin hydrophobic cavity, hydroxypropyl-β-cyclodextrin formed a stoichiometric 2 : 1 complex with fullerene, effectively enhancing the water solubility and biological activity of fullerene, and the encapsulation ratio of the prepared fullerene was calculated to be 79%. Results of oxygen radical absorbance capacity and pyrogallol autoxidation experiments showed high antioxidant activity displayed by the fullerene@HP-β-CD inclusion complex. The supramolecular inclusion was further co-assembled, using multiple hydrogen bonds and electrostatic interactions, with chitosan and bentonite to form a supramolecular hydrogel; this hydrogel was successfully used in antiglycation, with a glycation end products inhibition rate of 43.99% at a 10% sample concentration. Therefore, the fullerene-polysaccharide ternary co-assembly supramolecular hydrogel showed good antioxidant and antiglycation abilities, and the construction of the polysaccharide supramolecular hydrogel provided a new perspective for raw materials to consider in cosmetics applications.

1 Introduction

Fullerene are considered to have antioxidant and antiglycation effects due to its excellent abilities to adsorb free radicals.[1–3] However, due to its poor water solubility, its application *in vivo* is greatly limited. In order to solve this problem, scientists have made many efforts to increase the biological activity of fullerene.[4–6] Previously, Wang used amino-terminated poly(propylene glycol) and cyclodextrin to modify cyclodextrin-based polypseudorotaxanes and cross-linked them with gold nanoparticles to form a network of supramolecular aggregates, which was used to capture fullerenes in aqueous conditions and showed good ability to cleave DNA under light irradiation.[7] Chen used triphenyl Zn-porphyrin-modified β-cyclodextrins, adamantyl-modified hyaluronate and fullerene to construct supramolecular nanoparticles, which showed the ability to cleave DNA to the nicked form under light irradiation.[8] The above results showed that the introduction of cyclodextrins can

effectively improve the solubility of fullerene. Although there have been many studies on water-soluble macrocycles and fullerene supramolecular assemblies, there has been little reported research on supramolecular fullerene hydrogels.

To improve the fullerene loading rate, cyclodextrins serving as a class of macrocycles have been introduced into the hydrogels. Due to their external hydrophilicity and internal hydrophobic cavities, cyclodextrins can form inclusion complexes with various hydrophobic guests through host–guest interactions,[9–12] effectively improving the water solubility, stability, bioavailability, and control of the release of guest molecules.[13–15] On the other hand, the cyclodextrins inclusion complex can also interact with some macromolecules using multivalent interactions to form supramolecular assemblies.[16–19] For example, in previous work, chitosan–modified cyclodextrin (CS–CD) was synthesized and mixed with Ag⁺ at a suitable pH to obtain a stable hydrogel through supramolecular complexation, and then the anionic drug diclofenac sodium (DS) was loaded on the prepared hydrogel with the help of electrostatic interactions to form a host–guest inclusion complex. In addition, this gel material has been used in wound healing research.[20]

In our current work, hydroxypropyl-β-cyclodextrin (HP-β-CD) was complexed with fullerenes; this process not only effectively increased the solubility and biocompatibility of the fullerenes, but also retained the original biological functions of the fullerenes such as their antioxidant properties. To load and stabilize the inclusion complex more effectively and further enhance the

[a] School of Materials Science and Engineering, University of Science and Technology Beijing, Beijing 100083, China

[b] Cosmetics Tech Center, Chinese Academy of Inspection and Quarantine, Beijing 100176, China

[c] College of Chemistry, State Key Laboratory of Elemento-Organic Chemistry, Nankai University, Tianjin 300071, P. R. China. E-mail: chenyong@nankai.edu.cn, yuliu@nankai.edu.cn

† Electronic supplementary information (ESI) available. See DOI: https://doi.org/10.1039/d3sm00203a

‡ Contributed equally to this work.

antiglycation effect of the system, chitosan and bentonite were simply mixed together to prepare hydrogels and the inclusion complex was loaded into the hydrogel to form a stable ternary co-assembly supramolecular hydrogel. This fullerene-polysacc-haride supramolecular hydrogel showed several inherent advantages: (1) both chitosan and cyclodextrin being water soluble, biocompatible, and biodegradable; (2) the hydrogel being a kind of functional polymer material with high water content, good biocompatibility and being similar to natural biological tissue,[21] and (3) the combination of fullerene, cyclodextrin and chitosan being able to produce a resultant hydrogel showing multiple bioactivities such as antioxidation and antiglycation. Therefore, the formed supramolecular hydrogels were anticipated to have good application potential as cosmetics additives.[22] The antioxidant activity of the fullerene@HP-β-CD inclusion complex was tested using the oxygen radical absorbance capacity (ORAC) and pyrogallol autoxidation methods. In addition, the hydrogel showed good antiglycation ability with the production of glycation end products inhibited at a rate of 43.99% when using a 10% sample concentration, and should hence have potential application value in cosmetics and biomedicine Scheme 1.

2 Experimental

2.1 Preparation of the fullerene@HP-β-CD inclusion complex

A mass of 1 mg of fullerene was adequately ground using a mortar, and was then combined with 20 mg of HP-β-CD, with grinding continued on the resulting mixture. Samples of the ground mixture were each mixed with 10 mL of distilled water and each resulting mixture was either subjected to ultrasonic oscillation for 6 hours or stirred for 24 hours under the protection of inert gas. Each resulting solution was filtered using a disposable needle filter membrane with a pore size of 0.8 μm. The filtered solid precipitate was the unreacted fullerene, and the yellow solid obtained after lyophilization of the filtrate under essentially vacuum conditions was the fullerene@HP-β-CD inclusion complex (with the encapsulation ratio of fullerene calculated to be 79%).

2.2 Preparation of chitosan–bentonite hydrogel

A mass of 450 mg of bentonite was dissolved in 30 mL of distilled water, which was then stirred thoroughly until the

bentonite was evenly dispersed in the distilled water. Then the upper layer of the suspension was taken. Then a mass of 300 mg of chitosan was dissolved in 20 mL of 1% aqueous dilute acetic acid, to which 20 mL of the taken upper layer of the bentonite suspension was added and stirred overnight. A volume of 30 mL of an aqueous solution of 0.5 M sodium hydroxide was added into the chitosan–bentonite mixture, and the resulting mixture was stirred overnight. This stirred mixture was then filtered to obtain chitosan–bentonite gel, which was washed with copious amounts of distilled water, and then dialyzed with distilled water for more than 5 days to remove the excess sodium hydroxide. The chitosan–bentonite hydrogel was obtained by filtering the dialyzed solution.

### 2.3 Preparation of supramolecular hydrogels loaded with fullerene@HP-β-CD inclusion complexes

Supramolecular hydrogels loaded with fullerene@HP-β-CD inclusion complexes were obtained by dissolving 10 mg of the inclusion complexes in a small amount of distilled water and adding the aqueous inclusion complexes into 10 g of chitosan–bentonite hydrogels.

3 Results and discussion

β-CD has been previously shown to form a stoichiometric 2 : 1 inclusion complex with fullerenes.[23,24] In order to increase the solubility of fullerene and ensure the biocompatibility of the inclusion complex, HP-β-CD with a suitable cavity size and excellent water solubility was assembled with fullerenes. As shown in Fig. 1, the prepared fullerene@HP-β-CD inclusion complex formed a solid with a yellow color obviously different from the color of HP-β-CD or fullerene. In addition, thermo-gravimetry experiment results showed that the inclusion complex lost about 80% of its initial weight as the temperature was increased to 400 °C, whereas the HP-β-CD almost completely decomposed at this temperature. The change in color upon forming the inclusion complex and the results of the thermogravimetry experiments together confirmed the formation of the fullerene@HP-β-CD inclusion complex. Subsequently, the encapsulation efficiency of the fullerene@HP-β-CD inclusion complex was calculated from obtained UV-Vis spectra. By comparing the UV-Vis absorption intensity of C60 (0.02 g L^{-1} in cyclohexane) with that of the fullerene@HP-β-CD aqueous solution at their respective absorption peaks—*i.e.*, with the absorption peak of the fullerene–cyclohexane solution at 330 nm and that of the fullerene@HP-β-CD inclusion complex solution at 344 nm—the encapsulation ratio of the fullerene@ HP-β-CD inclusion complex was calculated to be 79%. That is, every 100 mg of fullerene@HP-β-CD inclusion complex contained 3.80 mg of fullerene. Based on this calculation, HP-β-CD was in excess in the fullerene@HP-β-CD system. This excess apparently shifted the host–guest binding equilibrium to the formation of the inclusion complex, and in the meanwhile inhibited its dissociation. As shown in Fig. S1 and S2 (ESI†), an obvious characteristic peak at 720 *m/z* was observed in the
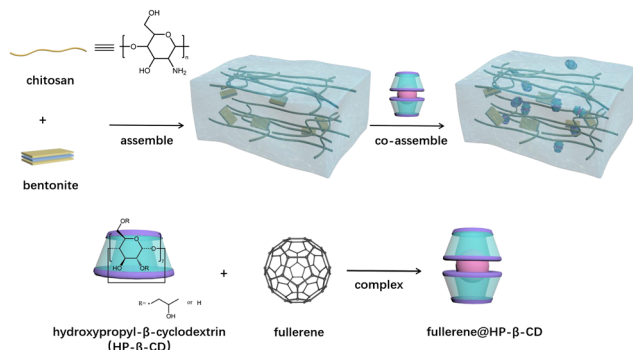
**Scheme 1** . Construction of a supramolecular hydrogel containing a fullerene@HP-β-CD inclusion complex.
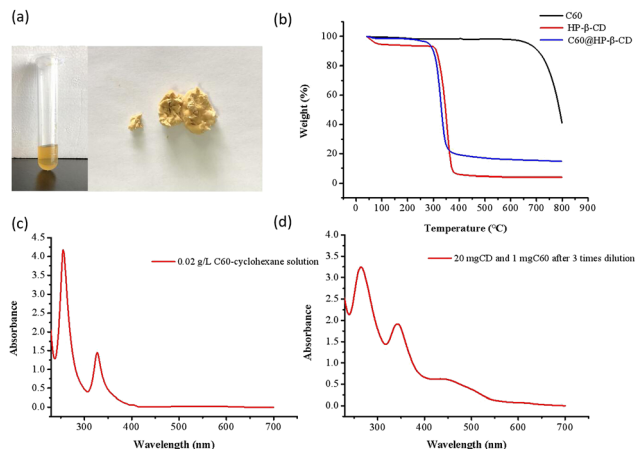
Fig. 1 (a) Photograph of an aqueous solution of the fullerene@HP-β-CD inclusion complex and a photograph of the lyophilized products. (b) Thermogravimetry curve of the fullerene@HP-β-CD inclusion complex. (c) UV spectrum of a cyclohexane solution of 0.02 g L^{-1} C60. (d) UV-Vis spectrum of an aqueous solution of fullerene@HP-β-CD prepared with 1 mg C60 and 20 mg HP-β-CD and then diluted 3 fold, to produce a final concentration of fullerene of 0.026 g L^{-1}.

Fig. 2 (a) Fluorescence quenching spectra of an AAPH-containing fluorescein solution. (b) Fluorescence quenching spectra of a fluorescein solution sample containing AAPH with HP-β-CD. (c) Spectrograms of the C60@HP-β-CD inclusion complex antioxidant effect tested by carrying out ORAC experiments. (d) Spectrograms of the C60@HP-β-CD inclusion complex antioxidant effect tested by carrying out pyrogallol autoxidation.

MALDI-TOF mass spectrum of fullerene@HP-β-CD but not in that of HP-β-CD, indicating the presence of fullerenes in the inclusion complex.

The antioxidant activity of the fullerene@HP-β-CD inclusion complex was tested by performing an oxygen radical absorbance capacity (ORAC) experiment,[25] the results of which are shown in Fig. 2. We used 2,2′-azobis(2-methylpropionamidine) dihydrochloride (AAPH) as a free radical initiator that has been shown to release free radicals at a temperature above 37 °C and to quench the fluorescence emission of fluorescein. Note that in general, antioxidants can absorb free radicals, thereby inhibiting the quenching of fluorescence by the free radicals. In the current work, the ORAC experiment was carried out in phosphate buffer solution (pH 7.4), and the concentrations of phosphate buffer, AAPH and fluorescein were 75 mmol L^{-1}, 12.8 mmol L^{-1} and 63 nmol L^{-1}, respectively. First, in order to prove the expected role of fullerene rather than of HP-β-CD as the source of antioxidant activity of the inclusion complexes, a control experiment was conducted. It was found that when only HP-β-CD was added into the AAPH solution, the rate of fluorescence quenching was basically consistent with that when nothing was added, indicating a lack of any antioxidant activity displayed by HP-β-CD. However, when fullerene@HP-β-CD was added to various samples of the system to make final fullerene@HP-β-CD concentrations of 0.1 g L^{-1}, 0.2 g L^{-1}, 0.3 g L^{-1} and 0.4 g L^{-1}, respectively (corresponding to fullerene contents of 3.8 mg L^{-1}, 7.6 mg L^{-1}, 11.4 mg L^{-1} and 15.2 mg L^{-1} respectively), the rate of fluorescence quenching by free radicals decreased, with greater extents of this decrease observed for higher fullerene@HP-β-CD concentrations. This result clearly demonstrated the ability of fullerene@HP-β-CD to remove free radicals, i.e., demonstrated its antioxidant activity.

The pyrogallol autoxidation method was also used to test the antioxidant activity of fullerene@HP-β-CD. In general,
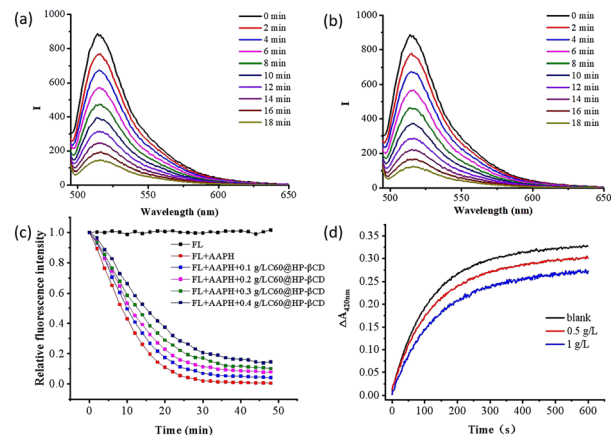
under alkaline conditions, pyrogallol produces superoxide free radicals for autoxidation, and the autoxidation products of pyrogallol can be detected using a UV-Vis spectrophotometer. With the autoxidation of pyrogallol, the absorption of light at wavelengths of 320 nm and 420 nm by the pyrogallol solution increases gradually. The addition of antioxidant can decrease the quantity of superoxide free radicals, thereby inhibiting the autoxidation of pyrogallol. In the current work, in a typical experiment carried out in 0.05 mol L^{-1} Tris–HCl buffer solution (pH 8.2), the concentration of pyrogallol was 2 mmol L^{-1}, and fullerene@HP-β-CD concentrations of 0.5 g L^{-1} and 1 g L^{-1} (corresponding to fullerene concentrations of 19 mg L^{-1} and 38 mg L^{-1}, respectively) were tested. In addition, 1 mmol L^{-1} disodium EDTA was added to the buffer solution to eliminate the influence of metal ions in the test. The increase, as a function of time, of the absorption of 420 nm-wavelength light by the pyrogallol solution was measured for each of various concentrations of fullerene@HP-β-CD added into the system. As shown in Fig. 2d, the autoxidation rate of pyrogallol with fullerene@HP-β-CD was measurably slower than that without fullerene@HP-β-CD, indicating that the fullerene@HP-β-CD displayed satisfactory antioxidant activity.

Subsequently, fullerene@HP-β-CD was loaded on hydrogels prepared from chitosan and bentonite. Due to chitosan being positively charged and bentonite negatively charged, they can form a stable hydrogel using electrostatic interactions. To test the stability of chitosan/bentonite hydrogels and fullerene@HP-β-CD-loaded hydrogels, their rheological properties were characterized using a rheometer. As shown in Fig. 3, when the fixed scanning frequency was 1 Hz, the storage modulus (G') of each of the two hydrogels was always greater than the loss modulus (G'') as the strain was increased from 0.1% to 100%. In the scanning frequency curve, when the fixed stress was 1.0%, the higher G' and lower G'' gradually increased in a
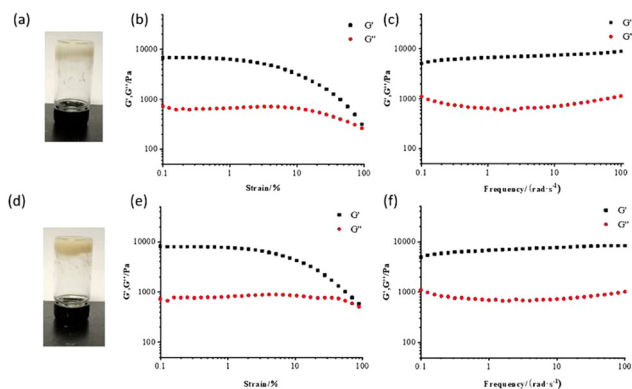
Fig. 3 (a) Photograph of a chitosan–bentonite hydrogel sample. (b) G' (storage modulus) and G'' (loss modulus) as functions of strain for the chitosan–bentonite hydrogel. (c) G' and G'' as functions of frequency for the chitosan–bentonite hydrogel. (d) Photograph of chitosan/bentonite hydrogel loaded with fullerene@HP-β-CD. (e) G' and G'' as functions of strain for the chitosan/bentonite hydrogel loaded with fullerene@HP-β-CD. (f) G' and G'' as functions of frequency for the chitosan/bentonite hydrogel loaded with fullerene@HP-β-CD.

Fig. 4 (a) Test results for antiglycation of chitosan/bentonite hydrogels. (b) Test results for antiglycation of fullerene@HP-β-CD-loaded chitosan/bentonite hydrogel. (Here, 1% aminoguanidine hydrochloride was used as positive control group).

nearly parallel fashion as the frequency was increased from 0.1 rad s^{-1} to 100 rad s^{-1}. These results illustrated the stability of the three-dimensional network in the hydrogel, the lack of damage to the three-dimensional structure of the hydrogel upon the loading of fullerene@HP-β-CD, and the fullerene@HP-β-CD-loaded hydrogel maintaining a stable gel performance.

An IR spectrum of the freeze-dried chitosan/bentonite xerogel is shown in Fig. S3a (ESI†), and IR spectra of original bentonite and chitosan are shown in Fig. S3b and c (ESI†). The spectrum of the xerogel showed O–H and N–H stretching vibration signals at 3450–3266 cm^{-1}, which were recognized as the characteristic IR signals of chitosan. Moreover, the spectrum of xerogel also showed the bending vibration signal of –OH at 1635 cm^{-1} and the stretching vibration signals of Si–O–Si at 1093 cm^{-1} and 1029 cm^{-1}, recognized as the characteristic IR signals of the bentonite structure. Therefore, the formation of the hydrogel from chitosan and bentonite was demonstrated by the IR spectrum of the freeze-dried chitosan/bentonite xerogel that presented the characteristic signals assigned to chitosan and bentonite. SEM images of chitosan/bentonite hydrogel and chitosan/bentonite hydrogel loaded with fullerene@HP-β-CD are shown in Fig. S4 and S5 (ESI†). Cross-linking between the bentonite sheet structure and chitosan through electrostatic interactions were observed in these images. The structure of the hydrogel remained stable after the addition of the fullerene inclusion compound.

Furthermore, the antiglycation abilities of these two hydrogels were assessed. In general, glycation end products (AGEs) generated in a glycation process show fluorescence characteristics, with an obvious fluorescence peak emission wavelength of 440 nm under an excitation wavelength of 370 nm. In the current work, AGEs were generated by incubating bovine serum protein in glucose. The mixed solution of bovine serum protein and the antioxidant hydrogel was incubated in phosphate buffer solution containing glucose, and then the fluorescence value of incubated
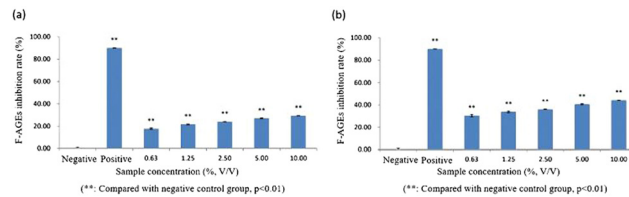
AGEs was measured. The inhibition effect of the antioxidant sample on the glycation reaction, *i.e.*, the antiglycation ability of the sample, was evaluated by using 1% aminoguanidine hydrochloride as the positive control group. As shown in Fig. 4, Fig. S6 and S7 (ESI†), both chitosan/bentonite hydrogel and fullerene@HP-β-CD-loaded chitosan/bentonite hydrogel showed good antiglycation ability, and the fullerene@HP-β-CD-loaded chitosan/bentonite hydrogel showed a higher antiglycation effect than did the chitosan/bentonite hydrogel without fullerene@HP-β-CD. In addition, antiglycation experiments using free HP-β-CD and fullerene@HP-β-CD were also performed (Fig. S8 and S9, ESI†). Here, the fullerene@HP-β-CD complex showed slight antiglycation (~0.5%), similar to that of free HP-β-CD but much lower than that of the chitosan/bentonite hydrogel. Therefore, we deduced a relatively small effect of the amount of fullerene@HP-β-CD inclusion complex on the antiglycation.

4 Conclusions

In conclusion, we used HP-β-CD and fullerenes to prepare a fullerene@HP-β-CD inclusion complex and further loaded it on chitosan/bentonite hydrogels. Owing to the solubilization ability of HP-β-CD and the antioxidation ability of fullerene, the resultant fullerene@HP-β-CD inclusion complex and the corresponding hydrogel exhibited good water solubility and antioxidation ability (for fullerene@HP-β-CD) as well as a good antiglycation effect (for hydrogel). Owing to these properties along with advantages of simple preparation and good biocompatibility, the fullerene@HP-β-CD inclusion complex and the corresponding hydrogel are expected to be used as raw materials in cosmetics with superior application prospects.

Conflicts of interest

There are no conflicts to declare.

Acknowledgements

Notes and references

1 H. W. Kroto, J. R. Heath, S. C. O'Brien, R. F. Curl and R. E. Smalley, *Nature*, 1985, **318**, 162–163.

2 P. D. Hale, *J. Am. Chem. Soc.*, 1986, **108**, 6087–6088.

3 P. J. Krusic, E. Wasserman, P. N. Keizer, J. R. Morton and K. F. Preston, *Science*, 1991, **254**, 1183–1185.

4 T. X. Zhang, J. J. Li, H. B. Li and D. S. Guo, *Front. Chem.*, 2021, **9**, 710808.

5 T. Braun, A. Buvaribarcza, L. Barcza, I. Konkolythege, M. Fodor and B. Migali, *Solid State Ionics*, 1994, **74**, 47–51.

6 D. Antoku, K. Sugikawa and A. Ikeda, *Chem. – Eur. J.*, 2019, **25**, 1854–1865.

7 Y. Liu, H. Wang, P. Liang and H. Y. Zhang, *Angew. Chem., Int. Ed.*, 2004, **43**, 2690–2694.

8 Y. Chen, D. Zhao and Y. Liu, *Chem. Commun.*, 2015, **51**, 12266.

9 H. Jin, L. Yang, M. J. R. Ahonen and M. H. Schoenfisch, *J. Am. Chem. Soc.*, 2018, **140**, 14178–14184.

10 C. Zhou, H. Wang, H. Bai, P. Zhang, L. Liu, S. Wang and Y. Wang, *ACS Appl. Mater. Interfaces*, 2017, **9**, 31657–31666.

11 W. Zhou, Y. Chen, Q. Yu, P. Li, X. Chen and Y. Liu, *Chem. Sci.*, 2019, **10**, 3346–3352.

12 M. Inouye, K. Hayashi, Y. Yonenaga, T. Itou, K. Fujimoto, T. A. Uchida, M. Iwamura and K. Nozaki, *Angew. Chem., Int. Ed.*, 2014, **53**, 14392–14396.

13 Z. Liu, X. Dai, Q. Xu, X. Sun and Y. Liu, *Chin. J. Chem.*, 2022, **40**, 493–499.

14 S.-S. Jia, W.-S. Xu, Y. Chen and Y. Liu, *Chin. Chem. Lett.*, 2021, **32**, 2773–2776.

15 Z. Liu, L. Ye, J. Xi, J. Wang and Z. Feng, *Prog. Polym. Sci.*, 2021, **118**, 101408.

16 X. M. Chen, Y. Chen, X. F. Hou, X. Wu, B. H. Gu and Y. Liu, *ACS Appl. Mater. Interfaces*, 2018, **10**, 24987–24992.

17 Z. Li, G. Wang, Y. Wang and H. Li, *Angew. Chem., Int. Ed.*, 2018, **57**, 2194–2198.

18 Y. J. Ooi, Y. Wen, J. Zhu, X. Song and J. Li, *Biomacromolecules*, 2020, **21**, 1136–1148.

19 J. Niu, Y. Chen and Y. Liu, *Soft Matter*, 2019, **15**, 3493–3496.

20 J. Wang, L. Feng, Q. Yu, Y. Chen and Y. Liu, *Biomacromolecules*, 2021, **22**, 534–539.

21 X. Lin, Y. Fang, Z. Hao, H. Wu, M. Zhao, S. Wang and Y. Liu, *Small*, 2021, **17**, 2103303.

22 G. Fang, X. Yang, S. Chen, Q. Wang, A. Zhang and B. Tang, *Coord. Chem. Rev.*, 2022, **454**, 214352.

23 C. N. Murthy and K. E. Geckeler, *Fullerenes, Nanotubes, Carbon Nanostruct.*, 2002, **10**, 91–98.

24 T. Gangadhar, V. I. Bhoi, S. Kumar and C. N. Murthy, *J. Inclusion Phenom. Macrocyclic Chem.*, 2014, **79**, 215–223.

25 J. Xu, X. Yao and Y. Li, *Chin. Pharmacol. Bull.*, 2006, **22**, 1015–1021.